

The sound of the event horizon

Roman Konoplya

Silesian University in Opava

roman.konoplya@gmail.com

based on:

JCAP 10 (2022) 091;

JCAP 07 (2023) 001;

Phys.Rev.D 107 (2023) 10, 104050;

Phys.Rev.D 108 (2023) 10, 104054;

Phys.Rev.D 107 (2023) 6, 064039

e-Print: 2209.00679,

Int.J.Mod.Phys.D 32 (2023) 14, 2342014

Prague,
September 23, 2024

Abstract and Summary

During the ringdown phase of a gravitational signal emitted by a black hole, the least damped quasinormal frequency dominates. If modifications to Einstein's theory induce noticeable deformations of the black-hole geometry only near the event horizon, the fundamental mode remains largely unaffected. However, even a small change near the event horizon can significantly impact the first few overtones, providing a means to probe the geometry of the event horizon. Overtones are stable against small deformations of spacetime at a distance from the black hole, allowing the event horizon to be distinguished from the surrounding environment. In contrast to echoes, overtones make a much larger energy contribution. These findings open up new avenues for future observations.

The fundamental mode

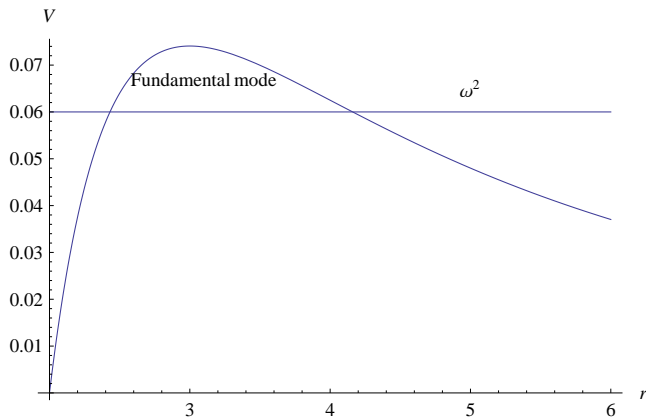


Figure: Rather symbolic effective potential for a Schwarzschild black hole; $M = 1$.

Small deformations near the event horizon I

The metric of a spherically symmetric black hole can be written in the following general form,

$$ds^2 = -N^2(r)dt^2 + \frac{B^2(r)}{N^2(r)}dr^2 + r^2(d\theta^2 + \sin^2\theta d\phi^2), \quad (1)$$

where r_0 is the event horizon, so that $N(r_0) = 0$. Following [L. Rezzolla, A. Zhidenko Phys.Rev.D 90 (2014) 8, 084009], we will use the new dimensionless variable $x \equiv 1 - r_0/r$, so that $x = 0$ corresponds to the event horizon, while $x = 1$ corresponds to spatial infinity. We rewrite the metric function N via the expression $N^2 = xA(x)$, where $A(x) > 0$ for $0 \leq x \leq 1$. Using the new parameters ϵ , a_0 , and b_0 , the functions A and B can be written as

$$\begin{aligned} A(x) &= 1 - \epsilon(1-x) + (a_0 - \epsilon)(1-x)^2 + \tilde{A}(x)(1-x)^3, \\ B(x) &= 1 + b_0(1-x) + \tilde{B}(x)(1-x)^2. \end{aligned} \quad (2)$$

Here the coefficient ϵ measures the deviation of r_0 from the Schwarzschild radius $2M$: $\epsilon = (2M - r_0)/r_0$.

Small deformations near the event horizon II

The coefficients a_0 and b_0 can be considered as combinations of the post-Newtonian (PN) parameters, $a_0 = (\beta - \gamma)(1 + \epsilon)^2/2$, $b_0 = (\gamma - 1)(1 + \epsilon)/2$. Current observational constraints on the PN parameters imply $a_0 \sim b_0 \sim 10^{-4}$, so that we can safely neglect them. The functions \tilde{A} and \tilde{B} are introduced through infinite continued fraction in order to describe the metric near the horizon (i.e., for $x \simeq 0$),

$$\tilde{A}(x) = \frac{a_1}{1 + \frac{a_2 x}{1 + \frac{a_3 x}{1 + \dots}}}, \quad \tilde{B}(x) = \frac{b_1}{1 + \frac{b_2 x}{1 + \frac{b_3 x}{1 + \dots}}}, \quad (3)$$

where a_1, a_2, \dots and b_1, b_2, \dots are dimensionless constants to be constrained from observations of phenomena which are localized near the event horizon. At the horizon only the first term in each of the continued fractions survives, $\tilde{A}(0) = a_1$, $\tilde{B}(0) = b_1$, which implies that near the horizon only the lower-order terms of the expansions are essential.

Small deformations near the event horizon III

When all the coefficients a_i , b_i and ϵ vanish, we have the Schwarzschild solution, so that one can consider the above parametrization as a general deformation of the Schwarzschild geometry. Then, we would like to understand which kind of deformations are responsible for the outburst of overtones. For this purpose, following [R. K. A. Zhidenko Phys.Rev.D 101 (2020) 12, 124004], we will distinguish the Schwarzschild-like *nonmoderate* black holes, whose metric functions are close to the Schwarzschild one everywhere except a small region near the event horizon in which it is strongly different. It is believed that this kind of black holes can be Schwarzschild mimickers, so that their ringdown profile and shadows are practically indistinguishable from those for the Schwarzschild ones. *Moderate* black holes are characterized by relatively slow change of the metric functions in the near horizon zone.

Small deformations near the event horizon IV

Overall, here we will compare the Schwarzschild black hole with the following four cases:

a) Nonmoderate Schwarzschild-like black hole with the Schwarzschild values of the Hawking temperature and radius of the event horizon (black hole 1).

b) Nonmoderate Schwarzschild-like black hole with considerably different (from the Schwarzschild one) Hawking temperature, but the same radius of the event horizon (black hole 2).

c) Moderate black hole with a slightly different radius, but the same mass and post-Newtonian behavior (black hole 3).

Thus, we study the moderate and nonmoderate near-horizon deformations of the Schwarzschild geometry.

After the separation of variables in the general covariant equations for the scalar and electromagnetic perturbations they can be reduced to the Schrödinger-like form,

$$\frac{\partial^2 \Psi}{\partial t^2} - \frac{\partial^2 \Psi}{\partial r_*^2} + V(r)\Psi = 0, \quad (4)$$

where the “tortoise coordinate” r_* is defined by the relation $dr_* = B(r)N^{-2}(r)dr$. The effective potentials for the scalar and electromagnetic fields are

$$V(r) = N^2(r) \frac{\ell(\ell+1)}{r^2} + \frac{1-s}{2r} \frac{d}{dr} \frac{N^4(r)}{B^2(r)},$$

where $\ell = 1, 2, \dots$ are the multipole numbers and $s = 0$ ($s = 1$) corresponds to the scalar (electromagnetic) field, respectively. The effective potential for the electromagnetic field has the form of the positive definite potential barrier, while this is not always so for a scalar field.

Quasinormal modes ω_n are frequencies corresponding to solutions of the master wave equation (4) with the requirement of the purely outgoing waves at infinity and at the event horizon,

$$\psi \propto e^{-i\omega t \pm i\omega r_*}, r_* \rightarrow \pm\infty.$$

In order to find QNMs we will use two methods: the time-domain integration and the Frobenius method.

In the time domain, we integrate the wavelike equation (4) in terms of the light-cone variables $u = t - r_*$ and $v = t + r_*$. using the discretization scheme of [C. Gundlach, R. Price, J. Pullin, Phys.Rev.D 49 (1994) 883-889] and, further, extracting QNMs with the Prony method.

In the frequency domain, after separating the time and radial coordinate, $\Psi(t, r) = e^{-i\omega t}R(r)$, we use the Frobenius method [E. Leaver, Proc.Roy.Soc.Lond.A 402 (1985) 285-298]. Namely, we express the function R , written with respect to the compact coordinate x , as a product of the factor, which diverges at the singular points $x = 0$ and $x = 1$ satisfying the QN boundary conditions, and the Frobenius series expansion

$$R(x) = x^{-i\omega/2\kappa_g} e^{i\omega r} x^\lambda \sum_{m=0}^{\infty} c_m x^m,$$

where $\kappa_g > 0$ and λ are determined by substituting the series into (4) and expanding, respectively, at $x = 0$ and $x = 1$.

By expanding the wavelike equation at $x = 0$, we find the recurrence relation for the coefficients c_m , which can be numerically reduced to the three-terms relation via Gaussian eliminations. Finally, we obtain an equation with the infinite continued fraction with respect to ω . In order to calculate the infinite continued fraction we use the Nollert improvement [Nollert, Phys.Rev.D 47 (1993) 5253-5258]. When the singular points of the wavelike equation appear within the unit circle $|x| < 1$, we employ a sequence of positive real midpoints as described in [Rostworowski, Acta Phys.Polon.B 38 (2007) 81-89].

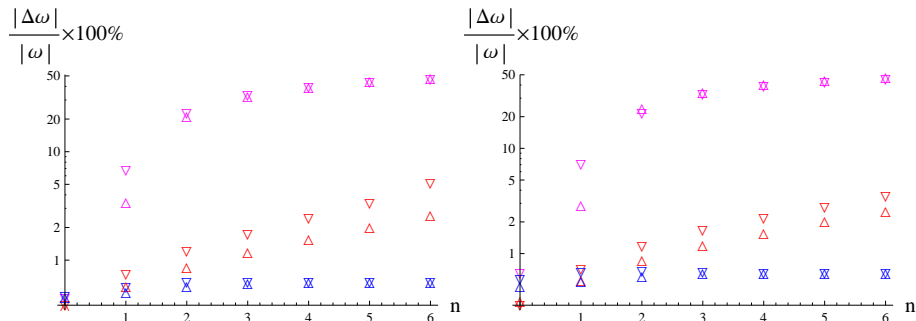


Figure: Relative deviation of first 7 qnms from the SBH ($\epsilon = 0$, $a_1 = b_1 = 0$, $T_H^{(0)} = 1/4\pi$) for the $s = 0$ (left) and $s = 1$ (right) perturbations $\ell = 1$ (∇) and $\ell = 2$ (Δ). For BH 1: $\epsilon = 0$, $a_1 = 0.0001$, $a_2 = -1000$, $a_3 = 1001$, $a_4 = 0$, $b_1 = 0$ ($T_H = 1.0001T_H^{(0)}$, red), BH 2: $a_1 = 0.5$, $a_2 = 100$, $a_3 = 0$, $b_1 = 0$ ($T_H = 1.5T_H^{(0)}$, magenta), BH 3: $\epsilon = -0.01$ ($2M = 1$, $a_1 = b_1 = 0$, blue).

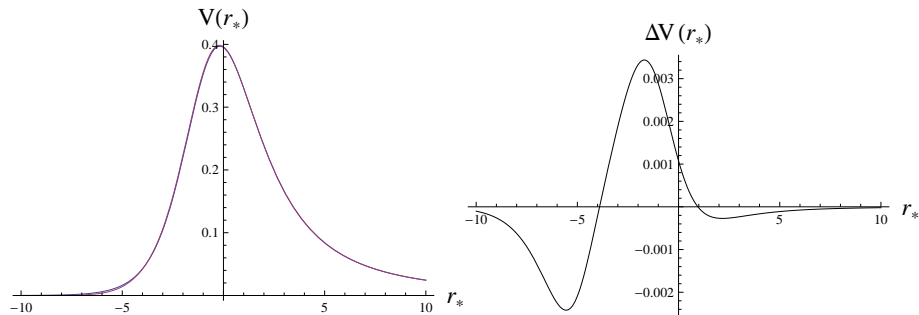


Figure: Left panel: Effective potentials ($s = 0, \ell = 1, r_0 = 2M = 1$) for the black hole 2 (blue) and Schwarzschild black hole (red) for comparison. Right panel: difference between the potentials.

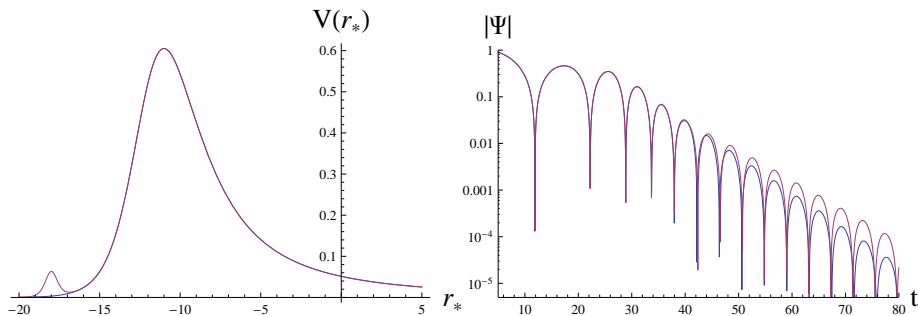


Figure: The effective potential and time-domain profile (at $r_* = 0$ corresponding to $r = 10$) for the $\ell = 2$ axial gravitational perturbations of the Schwarzschild ($r_0 = 2M = 1$) black hole (blue) and the potential deformed by a Poschl-Teller-like augmentation $\delta V = 0.06 / \cosh^2(2r_* + 36)$ (red).

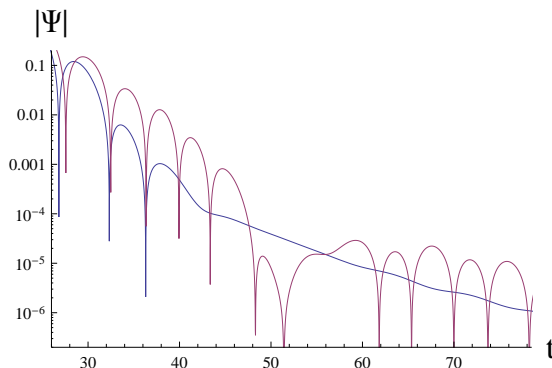


Figure: Time-domain profiles without the dominant-mode contribution, for SBH and $\omega_0 \approx 0.7622 - 0.1491i$ for the deformed potential. The amplitude, corresponding to the first overtone, is about four orders larger than the amplitude of the echo, appearing at $t \simeq 60$ (red). For an illustration, the augmentation is chosen to be large in order to compare the overtones effect with the echoes at earlier times.

The wave-like equation has the form,

$$\Delta(r)^s(r) \frac{d}{dr} \left(\Delta(r)^{1-s} \frac{dR}{dr} \right) + \left(\frac{K^2(r) - isK(r)\Delta'(r)}{\Delta(r)} + 4is\omega r - \lambda \right) R(r) = 0, \quad (5)$$

where $\Delta(r) \equiv (r^2 A(1 - r_0/r) + a^2)(1 - r_0/r)$, $K(r) \equiv (r^2 + a^2)\omega - am$, and λ is the separation constant. Here for the gravitational perturbations we consider $s = -2$. Then we consider ad hoc deformation of the wave-like equation for gravitational perturbations of Kerr black hole via deformations implemented in $A(x)$ (2). Requiring the parameter a_2 to be large, the effective potential will acquire deformation near the event horizon, but remain almost the same at a distance from the black hole.

In table 1 one can see that the same high sensitivity of overtones takes place for the near-horizon deformations of the equation for the gravitational perturbations of rotating black holes.

n	Kerr	modified Kerr
0	$0.586017 - 0.075630i$	$0.590393 - 0.075233i$
1	$0.577922 - 0.228149i$	$0.578766 - 0.226295i$
2	$0.562240 - 0.383895i$	$0.548651 - 0.391231i$
3	$0.538956 - 0.542888i$	$0.488262 - 0.616589i$
4	$0.506263 - 0.697962i$	$0.597420 - 0.814367i$
5	$0.486283 - 0.830803i$	$0.709014 - 0.975480i$
6	$0.499165 - 0.983084i$	$0.829156 - 1.138613i$
7	$0.506652 - 1.156708i$	$0.951035 - 1.299293i$

Table: Dominant modes of gravitational perturbations ($\ell = m = 2$) for the Kerr black hole $a = 0.8$, $M = 1$, $r_0 = 1.6$ ($\epsilon = 0.25$) compared to the modified Kerr ($a_1 = 0.5$, $a_2 = 100$, $a_3 = 0$).

An important question remains whether it is possible that a tiny perturbation of the effective potential in the far zone, owing to black holes environment, such as an accretion disk, also produces the outburst of overtones? If so, then it would be difficult to distinguish the latter from the near-horizon deformations. For this purpose as an example we consider a simple augmentation of the Schwarzschild potential which approaches zero at the horizon as

$$\delta V \propto (r - r_0)^h, \quad r \rightarrow r_0$$

and at infinity as

$$\delta V \propto r^{-a}, \quad r \rightarrow \infty$$

having the maximum value $\delta V_{max} = \delta/r_0^2$ at $r = r_m > r_0$,

$$\delta V = \frac{\delta}{r_0^2} \left(\frac{1 - r_0/r}{1 - r_0/r_m} \right)^h \left(1 + \frac{h}{a} \times \frac{r/r_m - 1}{r_m/r_0 - 1} \right)^{-a}. \quad (6)$$

We consider $\delta = 0.006$, which is two orders smaller than the height of the main Schwarzschild peak for $\ell = 2$. Note, that the maximum deformation is of the same order as the one considered in Table I of [Jaramillo, et. al. Phys.Rev.Lett. 128 (2022) 21, 211102]. Such astrophysically big deformation of the potential leads to very small corrections of the first several overtones (see Appendix B) and the corrections become even smaller if we shift the deformation farther from the black hole. Unlike the deformation considered in [Jaramillo, et. al. Phys.Rev.Lett. 128 (2022) 21, 211102], the deformation (6) by construction does not affect the near-horizon behaviour of the effective potential. Therefore we conclude that the phenomenon of the overtone outburst indeed happens due to deformations near the horizon.

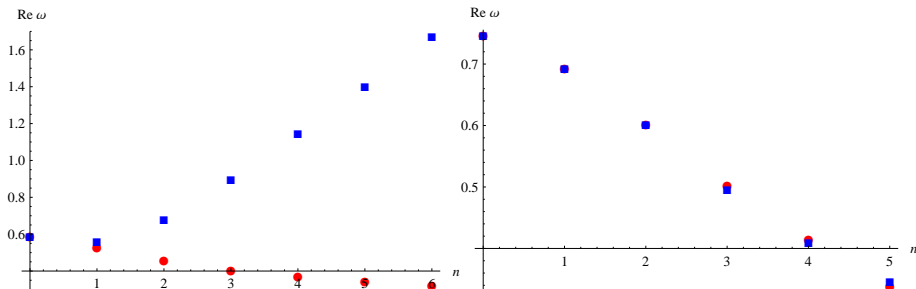


Figure: Left: The fundamental mode and first five overtones for the scalar field perturbations of the Schwarzschild black hole (red) and the black hole deformed in the near horizon zone (blue) as in fig. 3. Right: The first five modes of the gravitational Regge-Wheeler potential (red) and the potential deformed at a distance from the black hole (blue): $\delta = 0.006$ and $r_m = 20r_0$.

Conclusions

We have shown that a small deformation of the near-horizon geometry of a black hole leads to a strong change of overtones, while the fundamental mode remains almost unchanged. Thus the first few overtones can probe the event horizon geometry which potentially could be seen at the earlier stage of QN ringing [Giesler et. al. Phys.Rev.X 9 (2019) 4, 04106]. The observed here phenomenon of high sensitivity of lowest overtones to small deformations of the near horizon geometry is definitely connected with the so called “overtones instability” discussed in [Jaramillo, et. al. Phys.Rev.Lett. 128 (2022) 21, 211102]. There small perturbations of the effective potential were deformed by a sinusoidal function of the compact coordinate *not only near the event horizon, but in the whole space*. This approach does not allow one to understand which kind of deformations produce the outburst of overtones, which was the main question of our consideration. Here we have shown that *very small deformations solely near the event horizon are sufficient for such an outburst of overtones, while the deformations at a distance from the black hole need to be very large and physically irrelevant in order to produce a similar effect*.